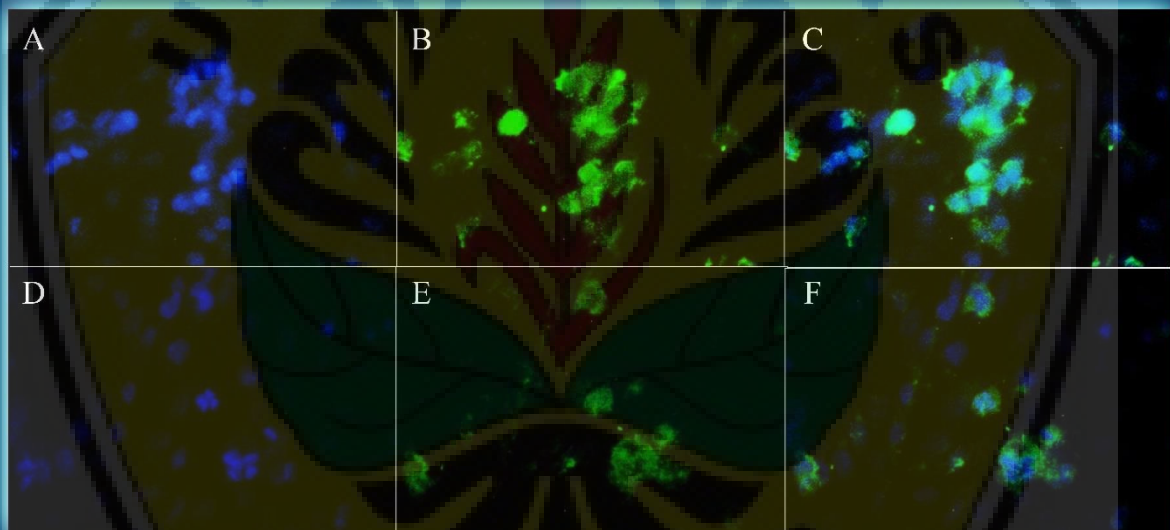


BI



# BiolImpacts



The DAPI staining and cyclin D1 protein detection in HT-29 cells treated with supernatant of probiotic *Lactobacillus rhamnosus*.  
A, B, and C: The untreated control cells. D, E, and F: The treated cells.  
A and D: Nuclei stained by DAPI. B and E: Stained cyclin D1 protein, C and F: Merged images of nuclei and cyclin D1 protein (Dehghani et al.).

## Editorial Board

Yadollah Omid (PharmD, PhD)Yadollah Omid (PharmD, PhD)

Founding Editor-in-Chief

Professor of Pharmaceutical Sciences

College of Pharmacy, Nova Southeastern University

Fort Lauderdale, Florida, USA

Jaleh Barar (PharmD, PhD)Jaleh Barar (PharmD, PhD)

Cofounding Editor-in-Chief

Professor of Pharmaceutical Cell Biology

Faculty of Pharmacy

Tabriz University of Medical Sciences

Tabriz, IRAN

Mohammad R. Rashidi (PharmD, PhD)Mohammad R. Rashidi (PharmD, PhD)

Director-in-Charge

Professor of Enzymology and Drug Metabolism

Faculty of Pharmacy

Tabriz University of Medical Sciences

Tabriz, IRAN

### *Editors*

Mohammad Rafi (PhD)Mohammad Rafi (PhD)

Professor of Neurology

Jefferson Medical College

Thomas Jefferson University

Philadelphia, USA

Assistant Professor,

Precision Health Program,

Michigan State University, USA

Amir Ali Hamidieh (MD)Amir Ali Hamidieh (MD)

Clinical Editor

Morteza Mahmoudi (PhD)Morteza Mahmoudi (PhD)

Professor of Pediatric Hematology Oncology,  
Stem Cell Transplantation

Faculty of Medicine, Tehran University of  
Medical Sciences

Tehran, IRAN

Khosro Adibkia (PharmD, PhD)Khosro  
Adibkia (PharmD, PhD)

Professor of Pharmaceutics

Faculty of Pharmacy

Tabriz University of Medical Sciences

Tabriz, IRAN

## *Associate Editors*

Abbas Alavi (MD)Abbas Alavi (MD)

Ali Khademhosseini (PhD)Ali  
Khademhosseini (PhD)

Mark Gumbleton (PhD)Mark Gumbleton  
(PhD)

Saghir Akhtar (PhD, MRPharmS)Saghir  
Akhtar (PhD, MRPharmS)

Moein Moghimi (PhD)Moein Moghimi (PhD)

Miguel Gama (PhD)Miguel Gama (PhD)

Robert C. Speth (MA, PhD, FAAAS, FAHA)

Miguel de la Guardia (PhD)Miguel de la  
Guardia (PhD)

Maurizio Scarpa (MD, PhD)Maurizio Scarpa  
(MD, PhD)

Dusan Losic (PhD)Dusan Losic (PhD)

Masahiro Sakagami (PhD)Masahiro Sakagami  
(PhD)

Faris Farassati (PharmD, PhD)Faris Farassati  
(PharmD, PhD)

Nokhodchi A. (PharmD, PhD)Nokhodchi A.  
(PharmD, PhD)

Hossein Nazemiyeh (PharmD, PhD)Hossein  
Nazemiyeh (PharmD, PhD)

Morteza Eskandani (PhD)Morteza Eskandani  
(PhD)

Alexander Seifalian (PhD)Alexander Seifalian  
(PhD)

Giulio Caracciolo (PhD)Giulio Caracciolo  
(PhD)

Marziyeh Fathi (PhD)Marziyeh Fathi (PhD)

## *Editorial Board*

Ghandehari H. (PhD)Ghandehari H. (PhD)

Abdollahi M. (PharmD, PhD)Abdollahi M.  
(PharmD, PhD)

Uchegbu I. (PhD)Uchegbu I. (PhD)

Hossein Omidian (PhD)Hossein Omidian  
(PhD)

Glassy M. (PhD)Glassy M. (PhD)

Fassihi R. (Ph.D.)Fassihi R. (Ph.D.)

Orhan I. (PhD)Orhan I. (PhD)

Mehvar R. (PharmD, PhD)Mehvar R.  
(PharmD, PhD)

Srinivasan Shanmugam (PhD)Srinivasan  
Shanmugam (PhD)

Jouyban A. (PharmD, PhD)Jouyban A.  
(PharmD, PhD)

# Digital Repository Universitas Jember

Maleki-Dizaji N. (PharmD, PhD)Maleki-Dizaji N. (PharmD, PhD)

Alok Bhushan (PhD)Alok Bhushan (PhD)

Sarker S.D. (PhD)Sarker S.D. (PhD)

Somi M.H. (MD)Somi M.H. (MD)

Kandalajt L. (PharmD, PhD)Kandalajt L. (PharmD, PhD)

Morris C. (PhD) Morris C. (PhD)

Hamidi M. (PhD)Hamidi M. (PhD)

Namazi H. (PhD) Namazi H. (PhD)

Ghafourian T. (PharmD, PhD)Ghafourian T. (PharmD, PhD)

Dastmalchi S. (PhD)Dastmalchi S. (PhD)

Movafeghi A. (PhD)Movafeghi A. (PhD)

Hadi Hamishehkar (Ph.D.)Hadi Hamishehkar (Ph.D.)

Razavi S.E. (PhD)Razavi S.E. (PhD)

Nadri S (PhD), Nadri S (PhD),

Barzegari A (PhD)Barzegari A (PhD)

Valizadeh H. (PharmD, PhD)Valizadeh H. (PharmD, PhD)

Jafar Ezzati Nazhad Dolatabadi (PhD)Jafar Ezzati Nazhad Dolatabadi (PhD)

Salmassi A. (PhD)Salmassi A. (PhD)

Davaran S. (PhD)Davaran S. (PhD)

Pavon-Djavid G. (PhD)Pavon-Djavid G. (PhD)

Shokri J. (PharmD, PhD)Shokri J. (PharmD, PhD)

Benboubetra M. (PhD)Benboubetra M. (PhD)

Hanaee J. (PharmD, PhD)Hanaee J. (PharmD, PhD)

Assi K. (PhD)Assi K. (PhD)

Farhoudi M. (MD)Farhoudi M. (MD)

Farnam AR. (MD)Farnam AR. (MD)

Norouzi P (PhD)Norouzi P (PhD)

Hamed Hamishehkar (PharmD, PhD)Hamed Hamishehkar (PharmD, PhD)

Pourseif M.M. (PhD)Pourseif M.M. (PhD)



## Contents

### In Press

1. Expression of functional eGFP-fused antigen-binding fragment of ranibizumab in *Pichia pastoris*  
Shirin Movaghar Asareh, Tahereh Savei, Sareh Arjmand, Seyed Omid Ranaei Siadat, Fataneh Fatemi, Mehrab Pourmadadi, Javad Shabani Shayeh
2. Fabrication, characterization, and optimization of a novel copper-incorporated chitosan/gelatin-based scaffold for bone tissue engineering applications  
Azam Bozorgi, Masoud Mozafari, Mozafar Khazaei, Mansooreh Soleimani, Zahra Jamalpoor
3. The active lung microbiota landscape of COVID-19 patients through the metatranscriptome data analysis  
Yang Han, Zhilong Jia, Jinlong Shi, Weidong Wang, Kunlun He
4. Brain targeted delivery of rapamycin using transferrin decorated nanostructured lipid carriers  
Fatemeh Khonsari, Mostafa Heydari, Rassoul Dinarvand, Mohammad Sharifzadeh, Fatemeh Atyabi
5. Molecular docking, molecular dynamics simulation, and ADMET analysis of levamisole derivatives against the SARS-CoV-2 main protease (MPro)  
Khalil EL Khatabi, Ilham Aanouz, Marwa Alaqrbeh, Mohammed Aziz Ajana, Tahar Lakhliifi, Mohammed Bouachrine
6. Intra-ovarian injection of bone marrow-derived c-Kit<sup>+</sup> cells for ovarian rejuvenation in menopausal rats  
Sepideh Sheshpari, Mahnaz Shahnazi, Shahin Ahmadian, Mohammad Nouri, Mehran Mesgari Abbasi, Rahim Beheshti, Reza Rahbarghazi, Ali Honaramooz, Mahdi Mahdipour
7. Osteoblastic cell response to Al<sub>2</sub>O<sub>3</sub>-Ti composites as bone implant materials  
Marjan Bahraminasab, Samaneh Arab, Somaye Ghaffari
8. Mesenchymal stromal cells therapy alone does not lead to the complete restoration of the skin parameters in diabetic foot patients within a 3-year follow-up period  
Nadezhda V. Maksimova, Anna V. Michenko, Olga A. Krasilnikova, Ilya D. Klabukov, Igor Yu. Gadaev, Michael E. Krashenninikov, Pavel A. Belkov, Aleksey V. Lyundup
9. On the issue of transparency on the internal investigation of academic bullying  
Morteza Mahmoudi, Sherry Moss, Loreleigh Keashly
10. Evaluation of in vitro fibroblast migration by electrospun triple-layered PU-CA/gelatin.PRGF/PU-CA scaffold using an AAVS1 targeted EGFP reporter cell line  
Forough Shams, Hamideh Moravvej, Simzar Hosseinzadeh, Bahram Kazemi, Masoumrh Rajabibazl, Azam Rahimpour
11. Gut microbial signature and gut-lung axis: A possible role in the therapy of COVID-19  
Ata Mahmoodpoor, Ali Shamekh, Sarvin Sanaie
12. The oncolytic activity of *Clostridium novyi* nontoxic spores in breast cancer  
Fatemeh Abedi Jafari, Asghar Abdoli, Reza Pilehchian, Neda Soleimani, Seyed Masoud Hosseini

13. A fuzzy logic-based computational method for the repurposing of drugs against COVID-19  
Yosef Masoudi-Sobhanzadeh, Hosein Esmaili, Ali Masoudi-Nejad
14. Nanoencapsulation of *Hirudo medicinalis* proteins in liposomes as a nanocarrier for inhibiting angiogenesis through targeting VEGFA in the Breast cancer cell line (MCF-7)  
Amir Shakouri, Housman Kahroba, Hamed Hamishekar, Jalal Abdolalizadeh
15. Simple monitoring of pH and urea in whole blood using wearable smart woman pad  
Bambang Kuswandi, Nur Andriani, Ari S Nugraha



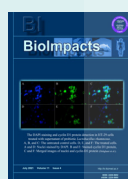


# Simple monitoring of pH and urea in whole blood using wearable smart woman pad

Bambang Kuswandi<sup>\*ID</sup>, Nur Andriani, Ari S Nugraha

Chemo and Biosensors Group, Faculty of Pharmacy, University of Jember, Jl. Kalimantan 37, Jember, 68121, Indonesia

## Article Info



**Article Type:**  
Original Article

### Article History:

Received: 12 Feb. 2020  
 Revised: 9 July 2020  
 Accepted: 12 July 2020  
 ePublished: 15 Aug. 2021

### Keywords:

Wearable device,  
 Smart woman pad,  
 Thread-paper microfluidic device,  
 pH,  
 Urea,  
 Whole blood

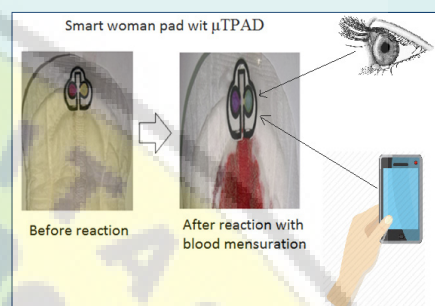
## Abstract

**Introduction:** In this work, we used a thread-paper microfluidic device ( $\mu$ TPAD) system, where a threaded part for the handling of the whole blood samples and a paper part for the reaction of plasma with immobilized bioreagents integrated into woman pad as a wearable sensing device namely as smart woman pad. The  $\mu$ TPAD as a wearable smart woman pad is developed for the detection of pH and urea in mensuration blood as real samples.

**Methods:** This combined device was constructed to cover the elements required, that is, separation of red blood cell, conditioning, analyte reaction, and colorimetric detection. The color change in sensing areas was measured in the RGB values via a smartphone using the Color Grab after a smart woman pad was used. The thread allowed red blood cell sampling and separation, while the paper microfluidic device was used for conditioning, biorecognition, and colorimetric transduction of pH and urea as analytes.

**Results:** The time needed for analysis was measured as 110 s using the equilibrium method for both analytes, with a limit of detection (LOD) of 72.55  $\mu$ g/mL for urea, with precision around 1.68%, while for pH around 0.80%. The smart woman pad allowed rapid detection of pH and urea in menstruation blood as real samples for monitoring of the kidney functions, and the results showed an agreement with the conventional methods that have been generally used in the clinical laboratory.

**Conclusion:** The smart woman pad has the potential to be used as a wearable device to monitor the health status of the user via its blood mensuration analysis.



## Introduction

Currently, in modern society, there is a trend to change the acquisition of chemical information from the standard laboratory to the place where it is required. This trend shifting approach is employed to acquire data from instrument-based methods that are centered in the laboratory, to become decentralized where user-based approaches are centered, namely distributed approaches.<sup>1</sup> One type of this analytical system is microfluidic device, often called lab-on-a-chip. This device relies on microfluidic platforms that allow for the chemical assay miniaturization so that it has the potential to serve rapid analysis.<sup>2</sup> Commonly, these devices work based on the capillarity action used in liquid propulsion, where it has advantages over other liquid propulsion systems, such as simplicity, rapid response, user-friendly, biocompatibility, and low cost. Developments of this device is mainly

based on paper, other materials, such as thread, and textile. Currently, they have been raised into a very active research area.<sup>1,3-5</sup> Coupled with smartphones that have color sensors, these microfluidic devices have promised to become a powerful micro total analysis systems ( $\mu$ TAS).<sup>6</sup> The  $\mu$ TAS should provide every element required to do analysis, such as sampling, sample transport and treatment, chemical reactions, detection, and information recording, including signal processing. These systems should be employed in the simplest way and user-friendly. These systems provide information that are easily understandable related to user needs.

The thread used has various benefits for the fabrication of analytical devices, such as path length, strength, materials, and small sample volume.<sup>7</sup> It has been employed as support for the microfluidic paper-based devices ( $\mu$ PAD) fabrication that can be used



\*Corresponding author: Bambang Kuswandi, Email: [b\\_kuswandi.farmasi@unej.ac.id](mailto:b_kuswandi.farmasi@unej.ac.id)



© 2021 The Author(s). This work is published by BioImpacts as an open access article distributed under the terms of the Creative Commons Attribution License (<http://creativecommons.org/licenses/by-nc/4.0/>). Non-commercial uses of the work are permitted, provided the original work is properly cited.

for numerous analytical applications, for example, as recognition support,<sup>8</sup> transduction reactions,<sup>9</sup> and reagent immobilization,<sup>10</sup> including sample conditioning<sup>11</sup> or separation, control, and flow manipulation.<sup>7,12</sup> In these methods, mainly the detection techniques are optical and electrochemical,<sup>13</sup> where the optical detection is the most common technique used. Besides its visual detection by nude eye, the acquisition of color images are performed by a smartphone<sup>14</sup> or a scanner<sup>15</sup> with further color image analysis.

In case of paper microfluidic devices coupled with thread, namely microfluidic thread-paper based analytical device ( $\mu$ TPAD),<sup>16</sup> they combine the fluid conductions by the thread, while the paper area used for the detection process with the subsequent color change is recorded by a smartphone or scanner. The  $\mu$ TPADs have been employed for glucose detection by enzymatic method, where a three-channel system is employed using nylon thread and chromatographic paper with three zones of reaction.<sup>16</sup> Other  $\mu$ TPAD systems have been reported for glucose and bovine serum albumin detection,<sup>17</sup> and glucose using a smartphone.<sup>18</sup>

In this work, we used a  $\mu$ TPAD system, where a threaded part was used for the handling of the whole blood samples and a paper part for the reaction of plasma with immobilized bioreagents integrated into the woman pad as wearable sensing device namely as smart women pad. Furthermore, the color change of the sensing area in the microfluidic paper-based device was performed by a smartphone using a free application (Color Grab). This opens the door to develop  $\mu$ TPAD as a wearable device by integrating into a woman pad to produce analytical data, which can improve significantly its versatility as an analytical tool. Thus, it could be beneficial for the woman user, since while they are wearing the pad, it could also monitor the pH and urea concentration via their mensuration blood based on the color change of the sensor. Besides, it benefits the producer that the pad can be upgraded to be smart by adding other functions, such as mensuration blood analysis in this case, without disturbing the pad main function. In the case of the urea and pH detection in whole blood, they need to separate the red blood cell from the plasma, which is achieved with a thread as a blood separation membrane and channel. In order to validate the results, the mensuration blood samples analysis from six women volunteers were analyzed using the smart woman pad, and the results were compared with the standard laboratory procedure for urea and pH using normal blood.

## Materials and Methods

### Reagents and solutions

Urease from jack bean (E.C.3.5.1.5), chlorophenol red (CPR), bromothymol blue (BTB), filter paper (Whatman no. 1), and phosphate buffer solution (1xPBS) consisting KCl, NaCl,  $\text{KH}_2\text{PO}_4$ , and  $\text{Na}_2\text{HPO}_4$  were obtained from

Sigma-Aldrich (MO, USA). All chemicals used are analytical reagent grade. All glassware used were washed using high pure water before use, and the solutions were also prepared using high pure water (resistance of  $18 \text{ M}\Omega\text{-cm}^{-1}$ ). Rubber-based ink (Sunrise, Indonesia) was ordered from Commanditaire Venootschap. Cipta Warna Jaya (Indonesia), food dyes, embroidery thread (Rose, Indonesia), cotton, sterile gauze (Onemed, Indonesia), and woman pad (Charm Body Fit, Indonesia) were obtained from Hypermart (Jember, Indonesia).

### Smart woman pad preparation

Before a  $\mu$ TPAD was prepared and integrated into a woman pad, first, a  $\mu$ PAD was fabricated using Whatman filter paper was patterned by the rubber base ink using screen printing technique in both sides of the paper ( $\mu$ PAD size  $160 \times 200 \text{ mm}$ ). After printing process, it was dried for 3 min using a hairdryer. The patterned paper became hydrophobic after it was dried, while the un-patterned part was still a hydrophilic paper. Afterword, the patterned paper was employed as  $\mu$ PAD for clinical analysis by immobilizing desired reagents to the sensing regions. For the urea detection, the sensing area was immobilized with urease along with BTB at optimized volume and concentration. While for pH, it was immobilized with CPR at optimized volume and concentration as well.

After the  $\mu$ PAD was fabricated, it was then attached into the woman pad by thread-stitching, where filter paper and sterile gauze were used as a microchannel for red blood cell separation, conditioning, and liquid sample propulsion through a capillarity action with the length of 10 cm and width of 1 cm. At the inlet of  $\mu$ PAD, it was also added with cotton around  $1 \text{ cm}^2$ , and  $\mu$ PAD was also stitched to the pad to fix its position in the pad (Fig. 1).

### Optimization of $\mu$ PAD reagent volume and concentration

To maximize the  $\mu$ PAD response toward analyte detection (urea and pH), the reagents used in the sensing areas need to be optimized to give a maximum response. The  $\mu$ PAD parameters that had been optimized were the maximum volume of  $\mu$ PAD and reagent volume used in the sensing

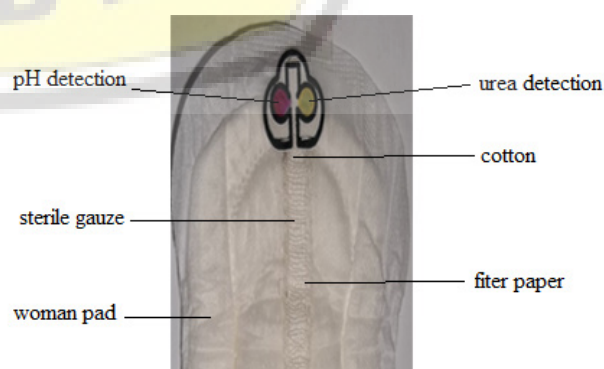


Fig. 1. Design of smart woman pad for detection of urea and pH of the mensuration blood sample.



area, including their concentration. Here for the  $\mu$ PAD volume, various volumes (10  $\mu$ L, 20  $\mu$ L, 30  $\mu$ L, 40  $\mu$ L, 50  $\mu$ L) were tested using red food dye, while its sensing area was tested with lower volumes (0.5  $\mu$ L, 1  $\mu$ L, 1.5  $\mu$ L, 2  $\mu$ L). For the concentration of reagents used (i.e. BTB and CPR), the concentration in the range of 1000–5000  $\mu$ g/mL was tested, while the urease used was fixed at 1 mg/mL and only the phosphate buffer solution was optimized in the pH range of 6.0 to 8.5.

### Apparatus

Digital images were obtained with a Samsung Note 5 smartphone (13 megapixels) (Samsung Electronics, Suwon, South Korea), installed on Android 5.1.1., using the Color Grab 3.6.1 (Loomatix®). The procedure was described in detail in previous work.<sup>19</sup> To take a stable and reproducible color image, the images were taken at a fixed distance (50 mm) from the smartphone to avoid the parallax error. Here, the smartphone flashlight was used along with an additional light called ‘Ringlight LED Clip-On for Smartphone’ (XY, China) that is usually used for a selfie, with the same distance and background, so that all the colors taken should be in a light-controlled area. For each image taken of the color change a sensor response to reduce and minimize ambient light effects that may result in false RGB obtained, which will affect the result of image analysis. Here, the algorithm of image-processing initially determines each color spot that has been taken, and then calculates the mean of several pixel intensities. Then, Color Grab® converted the image pixel intensity into an RGB value by its algorithm. Then, the  $\Delta$ mean RGB values presented as  $(\text{mean RGB}_{\text{conc.}} - \text{RGB}_{\text{Blank}})$  were plotted versus the pH or urea concentration in this case. Here the Color Grad application based on Android was used for simple data acquisition as it can be taken directly from a smartphone, compared with the ImageJ program that is usually used for color image analysis based on windows that needs a PC or laptop. While in terms of RGB, the sensor response is similar in RGB value obtained between both methods. In order to produce good reproducibility of the color response of the sensor, it needs to use the same camera with the same resolution to have a good relative standard deviation (RSD), since it is related to the color change that has been presented as RGB. In terms of the color change of the sensor response taken using the same camera with the same position and background, the RSD of ten-time measurements in terms of RGB was  $\leq 1\%$ .

### Blood samples

For the real blood sample, the mensuration blood was used. It was taken from six volunteer woman aged between 20 to 30 years old who were in the mensuration period between the days 1-3. They used the smart woman pad around 20 minutes and then the color change of  $\mu$ PAD was measured using  $\Delta$  mean RGB value as sensor response, and the urea content and pH of plasma were analyzed using the smart

woman pad. The determination of both analytes was done in triplicate using the linear equation constructed previously, while for the blood samples performed by the standard clinical lab that was carried out at the clinical laboratory of Dr. Soebandi Hospital (Jember) using vein blood as normal blood taken from the same six volunteer women.

### Measurement procedure

To use the smart woman pad, 10 mL of the simulated sample was deposited on the woman pad and left for 15 minutes until it reacted completely with the detection area for urea and pH or in the real situation, it could be used as a normal woman pad and left for 15 minutes until the plasma of mensuration blood was separated with the red blood cells, and reacted completely with the detection area for urea and pH. Afterward, a smartphone with the Color Grab was employed to capture the color change of the  $\mu$ PAD sensing area. To validate the  $\mu$ PAD results, the analyte concentrations found were compared to the standard method used in the clinical laboratory for pH and urea using a normal blood sample (vein blood). Here, we compared our results with the results obtained by the clinical laboratory from dr. Soebandi Hospital, Jember.

In this lab, pH was measured by pH meter (Orion Star A211 pH meter, UK) while urea was measured based on blood urea nitrogen (BUN). Each blood sample was measured 3 times. Here, BUN determines the urea nitrogen concentration in the blood sample. Since urea nitrogen is excreted by the kidneys from the blood, therefore high BUN concentrations could be related to kidney damage.<sup>20</sup> Here, the method was based on Beckman UniCel® DxC800 Synchron, where the DxC modular chemistry (BUNm) is used to determine the BUN concentration in serum or plasma by the method of enzymatic conductivity rate. A sample with precise volume is injected into a reaction cup consisting the urease and an electrode that responds to changes in the solution conductivity. Here, the conductivity increase rate is proportional directly to the concentration of urea in the sample.

## Results and Discussion

### Sensing mechanism

The smart woman pad as given in Fig. 1, as a combined device is constructed to cover all the analytical elements required, that is, separation red blood cell sample, conditioning, analyte recognition, and colorimetric detection. Here, the color change in sensing areas was captured with a smartphone and presented as the RGB values by using Color Grab, a free application, after a smart woman pad was used. The thread (10 cm length) that allows red blood cell sampling and separation from plasma, was combined between filter paper and sterile gauze that stitched with a thread to woman pad, wherein the inlet into  $\mu$ PAD was covered with a cotton pad to hold of any red blood cell entry into the  $\mu$ PAD so

that it only allows drawing the plasma into the  $\mu$ PAD, where conditioning, biorecognition and colorimetric transduction of pH and urea occur.

The pH detection is based on CPR response in terms of its color change toward the pH of the plasma from red to violet, while the urea detection is based on the enzymatic hydrolysis of urea by urease, in which ammonia was produced, where the ammonia could be detected by BTB. Here, the color change of the sensing area from yellow to blue in the presence of ammonia is correlated with urea concentration in the plasma (Fig. 2).<sup>21</sup> Thus, based on this sensing mechanism, the analysis of mensuration blood in a woman could be possible by using the plasma of mensuration blood, after it was separated from the red blood cells, and flowing the plasma toward  $\mu$ PAD to react completely with the detection area for urea and pH. All of the processes need time around 15 minutes, where it takes around 10 to 12 minutes to draw the plasma into the  $\mu$ PAD. The time taken for the sensor response is comparable with others.<sup>22,23</sup> Afterward, a smartphone with the Color Grab app was used to capture the color change.

#### Optimization of $\mu$ PAD

The maximum volume of  $\mu$ PAD was determined by flowing the red dye solution into the  $\mu$ PAD ranging from 10  $\mu$ L to 50  $\mu$ L. It was found that the  $\mu$ PAD has a maximum sample volume at 50  $\mu$ L (Fig. S1a). This sample volume (50  $\mu$ L) was used as a maximum sample volume for further experiments. Regarding the maximum volume for sensing area of  $\mu$ PAD, similarly, it was determined by drawing using red dye solution into sensing area ranging from 0,5  $\mu$ L to 2  $\mu$ L. It was found that both sensing area has a maximum sample volume at 2  $\mu$ L (Fig. S1b). This volume (2  $\mu$ L) was used for the volume of reagent used for reagent immobilization via the adsorption method in both sensing areas.

For reagent concentration optimization such as pH using

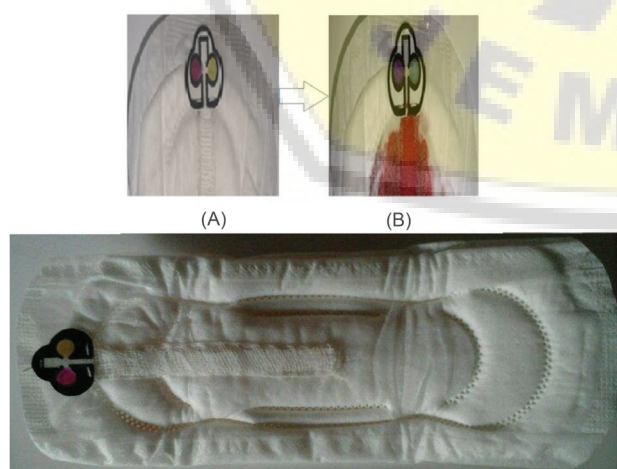


**Fig. 2.** The response of smart woman pad for detection of urea and pH of the mensuration blood sample, (A) before and (B) after reaction toward pH and urea.

CPR, it was optimized using various concentrations of CPR ranging from 1000 to 5000  $\mu$ g/mL, then it was tested with buffer pH 7.0 to find the maximum color change. It was found that 5000  $\mu$ g/mL CPR concentration gave the highest intensity color change toward pH 7 (Fig. S2a) and this concentration was used for further pH detection. Similarly, for BTB that was used along with urease at desired pH of 7.5 for urea detection, it was optimized using various concentrations of BTB ranging from 1000 to 5000  $\mu$ g/mL. Then, it was reacted with an urea standard at 1000  $\mu$ g/mL. Afterward, the BTB color change from yellow to blue color was compared to find the highest color change intensity. It was found that the concentration of BTB at 3000  $\mu$ g/mL gave a high-intensity color change similar to other concentrations such as 4000 and 5000  $\mu$ g/mL (Fig. S2b). Therefore, this BTB concentration (3000  $\mu$ g/mL) was then used for further measurements.

Besides BTB concentration optimization, another parameter that affected urea detection is pH. Therefore, the pH condition in the sensing area was optimized using phosphate buffer solution in the pH range from 6.0 to 8.5. Here, the BTB was used in optimized concentration (3000  $\mu$ g/mL) and reacted toward urea standard at 1000  $\mu$ g/mL. It was found that the pH was optimum at 7.5 where it gave the highest intensity color change compared to another pH (Fig. S2c). This pH was found to be suitable as a normal pH found in the real blood sample.<sup>24</sup> Therefore, this pH (7.5) has been selected to be used for further measurements.

#### Analytical figures toward pH

The response time of  $\mu$ PAD toward pH detection was performed by measuring the color change of immobilized CPR (conditioned at pH 7.0) from pink as its base color to become red-purple when it reacted with a phosphate buffer solution at pH 7.5. The time response was measured using a stopwatch, and it was found that the time response toward pH was found as the average of three measurements at 112 seconds or 1.86 minutes. This can be stated that this response time is adequate to be applied in a smart woman pad for pH detection. Since this pH response time is comparable to the response time for pH in a urine sample,<sup>25</sup> therefore around 2 minutes, in this case, was enough time for detection of pH in terms of color change using the proposed method.

The linear range of  $\mu$ PAD toward pH was determined by testing with a phosphate buffer solution at various pH, ranging from pH 4.0 to 7.5 as given in Table S1 and presented as linear range as presented in Fig. 3. According to Table S1, it can be determined that the higher the pH, the higher intensity of color change ( $\Delta$  mean RGB), so that the calibration curve also gives a positive correlation between the sensing response and pH, where the higher pH gives higher response as shown in Fig. 5, where the regression equation was found  $y = 5.9895 \text{ pH} - 21.544$  with a correlation coefficient ( $r$ ) value of 0.996. This value is

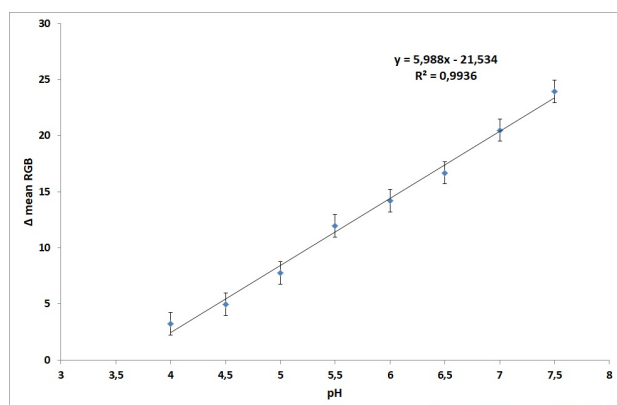


**Fig. 3.** The calibration curved of pH sensing of  $\mu$ PAD in the pH range 4.0 to 7.5 using phosphate buffer solution.

classified as an excellent correlation ( $\geq 0.99$ ) for this type of pH measurement.<sup>26</sup> While the precision of pH detection was performed toward phosphate buffer at pH 7.0 (6 samples) as normal pH for plasma or serum,<sup>27</sup> using the regression equation, and the results of pH detection was found to be excellent (RSD value was 0.79%), and this value was fulfilled for good precision value that requires RSD < 2%.<sup>26</sup>

#### Analytical figures toward urea

The response time of the sensing area of  $\mu$ PAD towards urea was measured by determining the color change of urea sensing (conditioned at pH 7.5) from yellow as its base color to become blue when it reacted with the urea standard solution (1000  $\mu$ g/mL). The time response was measured using a stopwatch, and it was found that the time response toward urea was found as the average of three measurements at 106 seconds or 1.76 minutes. This response time toward urea is adequate to be applied in the smart woman pad since the response time is not much different from the response time for pH detection (112 seconds or 1.86 minutes).

The linear range of  $\mu$ PAD toward urea was determined by reacting with various urea standard solution concentrations in the range from 100 to 2000  $\mu$ g/mL as given in Table S2 and presented as a linear range with a correlation coefficient ( $r$ ) value of 0.988 as given in Fig. 4 (inset). According to Table S2, it can be determined that the higher urea concentration, it can give a higher intensity of color change ( $\Delta$  mean RGB) so that the calibration curve gives a positive correlation between the sensing response ( $\Delta$  mean RGB) toward urea concentration. However, the best linear range was achieved in the concentration range between 100 to 800  $\mu$ g/mL as shown in Fig. 4, where regression equation was  $y = 0.0201 [\text{urea}] + 0.6968$  with a correlation coefficient ( $r$ ) value of 0.995. This value can be classified as an excellent coefficient value ( $\geq 0.99$ ) for this type of urea measurement.<sup>20</sup> Based on the regression equation, the limit of detection (LOD) ( $3\sigma$  of blank) was calculated to be 72.552  $\mu$ g/mL, while the limit

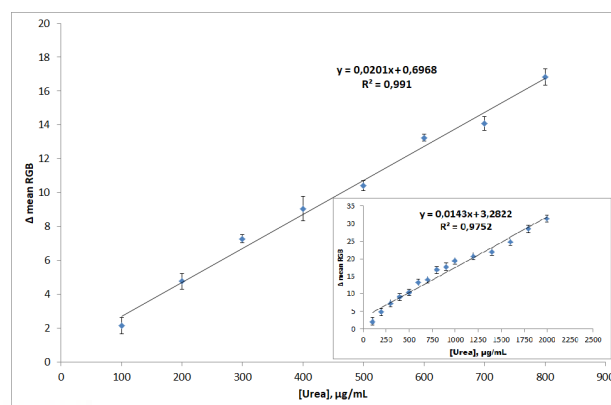


**Fig. 4.** The calibration curved of urea sensing of  $\mu$ PAD in the urea concentration range of 100 to 800  $\mu$ g/mL and 100 to 2000  $\mu$ g/mL (inset).

of quantification ( $10\sigma$  of blank) was found to be 241.838  $\mu$ g/mL. This value was adequate for the detection of urea in plasma or serum since the normal range of BUN is 5 to 20 mg/dL<sup>28</sup> or 500 to 2000  $\mu$ g/mL. In addition, a BUN over this level ( $>2000$   $\mu$ g/mL) would indicate an impaired function of the kidney significantly for a woman.<sup>20</sup>

The precision of urea was detected toward the urea standard solution at 140  $\mu$ g/mL (6 samples) just above the LOD of the  $\mu$ PAD, and by using the regression equation, and the results of urea detection was found to be excellent (RSD value was 1.68%), and this value was fulfilled for good precision value that requires RSD < 2%.<sup>26</sup> For the determination of accuracy, using the urea standard solution at 140  $\mu$ g/mL was performed by the addition of 80%, 100%, and 120% of the standard urea solution. Based on the regression equation for urea, it was found that the recovery values (%recovery) for the addition of 80%, 100%, and 120% were found to be 95.543%, 100.592%, and 98.143%, respectively. This accuracy values (% recovery) were fulfilled for the good accuracy or recovery between 90%-107%.<sup>26</sup>

The selectivity of the urea sensor was tested using NaCl, glucose, and creatinine as these compounds usually consist of the blood plasma. The urea sensing was tested toward 100  $\mu$ g/mL in the ratio 1:10 with these interferences. The results showed that no significant interference was found in this urea detection, since these interferences only give different responses less than 1%, and this interference can be negligible. Thus, it can be stated that the urea sensing of the  $\mu$ PAD is very selective toward urea detection.

In order to show the figure of merit of the proposed method, Table 1 shows the comparison of the results of other  $\mu$ PAD for the detection of urea in clinical samples, where the proposed method is comparable with others using urine samples, and better for urine determination using saliva in terms of LOD, and blood serum in terms of wider linear range. The detail of data in terms of biosensing mechanism used by others related to Table 1 is given in Table S3. Thus, this data shows that the proposed method in terms of smart woman pad, as a wearable

**Table 1.** The comparison of results between  $\mu$ PAD for the detection of urea in clinical samples

Sample	Figures of merit	Method	References
Urine	LOD: 1.02 mM (6.12 mg/dL) LR: 0–50 mM (0-300 mg/dL) r: 0.988	Fluorimetric	25
Saliva	LOD: 10.4 mg/dL LR: 10–260 mg/dL r: 0.960	Colorimetric	29
Blood serum	LOD: n.d. LR: 10-100 mg/dL r: 0.995	Colorimetric	30
Blood mensuration	LOD:72.552 $\mu$ g/mL (7.26 mg/dL) LR:100-2000 $\mu$ g/mL(10-200 mg/dL) r: 0.988	Colorimetric	This work

Note: LOD = limit of detection; LR = Linear range; n.d = not determined.

device could have also better figures of merit compared to other  $\mu$ PADs as the direct analytical tools using common analytical samples. Moreover, this wearable device demonstrated that  $\mu$ PAD can be integrated into woman pad to monitor the health status of the user via its blood mensuration samples, such as urea for monitoring of the kidney functions with good analytical performances.

### Applications

The applicability of the smart woman pad was evaluated using spiked samples, where a normal blood sample was added with a standard urea solution in 1:1 ratio with the urea concentration between 100-800  $\mu$ g/mL, and also with various pH of phosphate buffer solution between pH 4.0 to 7.5, and the results were summarized in Table 2. According to Table 2, the smart woman pad showed a different response (color change) as mean RGB value decreased toward different pH and urea concentrations,

where the higher urea concentration within the sample, the higher intensity of blue color in the urea sensing was shown, while in the case of pH, at pH 4.0 and 4.5 showed a dark yellow change to yellow, and at pH 5.0 to 7.5 showed red change to purple color. This can be stated that the color change that the smart woman pad is working well with the blood sample, where the plasma could be separated from the red-blood-cell within around 15 minutes until it reacts in both sensing areas for pH and urea. The time taken for the sensor response is comparable with others.<sup>5,22,23</sup> In addition, the  $\mu$ PAD color change using plasma shows similar color change compared to standard urea solution and standard buffer solution. Therefore, the linear equation constructed using buffered urea standard solution could also be applied for real sample using blood mensuration, since only the plasma is used in the detection for urea and pH.

For real sample analysis using blood mensuration, the

**Table 2.** The results of urea and pH detection using spiked samples

[Urea] $\mu$ g/mL and buffer added	$\mu$ PAD			Mean RGB value	
				Urea	pH
100 pH 4.0				163.366 $\pm$ 1.850	148.966 $\pm$ 1.331
200 pH 4.5				161.574 $\pm$ 1.058	147.245 $\pm$ 1.993
300 pH 5.0				157.963 $\pm$ 1.682	142.571 $\pm$ 1.897
400 pH 5.5				156.217 $\pm$ 1.819	141.145 $\pm$ 1.182
500 pH 6.0				155.176 $\pm$ 1.381	136.981 $\pm$ 1.957
600 pH 6.5				152.771 $\pm$ 0.987	132.458 $\pm$ 0.988
700 pH 7.0				151.841 $\pm$ 1.094	131.295 $\pm$ 1.238
800 pH 7.5				149.751 $\pm$ 1.321	130.771 $\pm$ 1.978

## Research Highlights

### What is the current knowledge?

✓ During the last decade, paper-based microfluidics offers promising applications in clinical analysis of biological fluids, including point of care devices.

✓ The application of paper-based microfluidics combined with other platforms as the wearable analytical device is still limited.

### What is new here?

✓ The proposed wearable analytical device is a simple, disposable, efficient, and cost-effective device for whole blood analysis.

✓ There is no need for complex instrumentation system since it can be detected using the naked eye or smartphone.

✓ This wearable analytical device can be applied to monitor the health status of the user via its blood mensuration analysis, such as pH and urea for monitoring the kidney functions.

smart woman pad was applied to the patient woman, where they wore the smart woman pad around 20 minutes and then the color change of  $\mu$ PAD was measured using  $\Delta$  mean RGB value as sensor response, and urea and pH of plasma were determined. The smart woman pad results were then compared with the results from the clinical laboratory of Dr. Soebandi Hospital, Jember, using normal blood as BUN, and the results are also given in Table 3, as a comparison. Based on the samples from the same six women donor, it can be stated that both results of the smart woman pad and clinical Laboratory were in good agreement in the determination of urea and pH. Thus, it can be stated that the smart woman pad can be used as an alternative wearable device in the detection of urea and pH of mensuration blood sample, which can also be used as early detection of kidney function. Therefore, the health monitoring condition could be performed easily by the user itself without the need to take a blood sample from them.

## Conclusion

A wearable smart woman pad consisting an  $\mu$ TPAD has been developed for the detection of pH and urea in a mensuration blood sample. The smart woman pad enables all the analytical tasks required, such as separation of red blood cell, conditioning, analyte reaction, and colorimetric detection using a smartphone via a free application (Color Grab). The smart woman pad allows rapid detection of pH and urea in the menstruation blood sample that can be used for early detection of the kidney functions, and the results show an agreement with the conventional methods that are generally used in the clinical laboratory using normal blood. Thus, it can be concluded that the smart woman pad has the potential to be used as a wearable sensing device to monitor the health status of the user via its blood mensuration analysis.

## Acknowledgments

This work was supported by Ditlitabmas, The Ministry of Research, Technology and Higher Education, the Republic of Indonesia through the World Class Research Grant 2019-2020.

## Funding sources

The World-Class Research Grant 2019-2020, The Ministry of Research, Technology and Higher Education, the Republic of Indonesia.

## Ethical statement

All the experiments in this work were done in compliance with the guidelines and regulations of the Ethical Committee of Clinical Research, the University of Jember, and all experiments were performed based on institutional guidelines. In addition, informed consent for participation in real sample analysis was obtained. At the same time, all the human individuals involved were informed about the research and they voluntarily agreed.

## Competing interests

The authors declare that they have no competing interests.

## Authors' contribution

BK supervised the work, NA performed the experimental work, ASN gathered the data, BK, NA, and ASN drafted the manuscript. BK finalized the manuscript.

## Supplementary Materials

Supplementary file 1 contains Tables S1-S3 and Figures S1-S2.

## References

1. Hoekstra R, Blondeau P, Andrade FJ. Distributed electrochemical sensors: recent advances and barriers to market adoption. *Anal Bioanal Chem* **2018**; 410: 4077-4089. <https://doi.org/10.1007/s00216-018-1104-9>
2. Mark D, Haeberle S, Roth G, von Stetten F, Zengerle R. Microfluidic lab-on-a-chip platforms: requirements, characteristics and applications. *Chem Soc Rev* **2010**; 39: 1153. <https://doi.org/10.1039/b820557b>
3. Akyazi T, Basabe-Desmouts L, Benito-Lopez F. Review on microfluidic paper-based analytical devices towards commercialisation. *Anal Chim Acta* **2018**; 1001: 1-17. <https://doi.org/10.1016/j.aca.2017.11.010>
4. Aydindogan E, Guler Celik E, Timur S. Paper-Based Analytical Methods for Smartphone Sensing with Functional Nanoparticles: Bridges from Smart Surfaces to Global Health. *Anal Chem* **2018**; 90: 12325-12333. <https://doi.org/10.1021/acs.analchem.8b03120>
5. Farajikhah S, Cabot JM, Innis PC, Paull B, Wallace G. Life-Saving Threads: Advances in Textile-Based Analytical Devices. *ACS Comb Sci* **2019**; 21: 229-240. <https://doi.org/10.1021/acscombsci.8b00126>
6. Boonyasit Y, Chailapakul O, Laiwattanapaisal W. A multiplexed three-dimensional paper-based electrochemical impedance device for simultaneous label-free affinity sensing of total and glycated haemoglobin: The potential of using a specific single-frequency value for analysis. *Anal Chim Acta* **2016**; 936: 1-11. <https://doi.org/10.1016/j.ACA.2016.05.047>
7. Nilghaz A, Ballerini DR, Shen W. Exploration of microfluidic devices based on multi-filament threads and textiles: A review. *Biomicrofluidics* **2013**; 7: 051501. <https://doi.org/10.1063/1.4820413>
8. Wu T, Xu T, Xu L-P, et al. Superhydrophilic cotton thread with temperature-dependent pattern for sensitive nucleic acid detection. *Biosens Bioelectron* **2016**; 86: 951-957. <https://doi.org/10.1016/j.bios.2016.07.041>
9. Liu R, Liu C, Li H, Liu M, Wang D, Zhang C. Bipolar electrochemiluminescence on thread: A new class of electroanalytical sensors. *Biosens Bioelectron* **2017**; 94: 335-343. <https://doi.org/10.1016/j.bios.2017.03.007>
10. Galpothdeniya WIS, McCarter KS, De Rooy SL, et al. Ionic liquid-based optoelectronic sensor arrays for chemical detection. *RSC Adv* **2014**; 4: 7225-7234. <https://doi.org/10.1039/C3RA47518B>

11. Ulum MF, Maylina L, Noviana D, Wicaksono DHB. EDTA-treated cotton-thread microfluidic device used for one-step whole blood plasma separation and assay. *Lab Chip* **2016**; 16: 1492-1504. <https://doi.org/10.1039/C6LC00175K>
12. Li H, Steckl AJ. Paper Microfluidics for Point-of-Care Blood-Based Analysis and Diagnostics. *Anal Chem* **2019**; 91: 352-371. <https://doi.org/10.1021/acs.analchem.8b03636>
13. Malon RSP, Heng LY, Córcoles EP. Recent developments in microfluidic paper-, cloth-, and thread-based electrochemical devices for analytical chemistry. *Rev Anal Chem* **2017**; 36. <https://doi.org/10.1515/revac-2016-0018>
14. Erenas MM, de Orbe-Payá I, Capitan-Vallvey LF. Surface Modified Thread-Based Microfluidic Analytical Device for Selective Potassium Analysis. *Anal Chem* **2016**; 88: 5331-5337. <https://doi.org/10.1021/acs.analchem.6b00633>
15. Brink C, Joubert T-H. Colorimetric detection for paper-based biosensing applications. *Proc. SPIE 10036, Fourth Conference on Sensors, MEMS, and Electro-Optic Systems* **2017**: 100360I. <https://doi.org/10.1117/12.2245448>
16. Lee W, Gonzalez A, Arguelles P, Guevara R, Gonzalez-Guerrero MJ, Gomez FA. Thread/paper- and paper-based microfluidic devices for glucose assays employing artificial neural networks. *Electrophoresis* **2018**; 39: 1443-1451. <https://doi.org/10.1002/elps.201800059>
17. Neris NM, Guevara RD, Gonzalez A, Gomez FA. 3D Multilayered paper- and thread/paper-based microfluidic devices for bioassays. *Electrophoresis* **2019**; 40: 296-303. <https://doi.org/10.1002/elps.201800383>
18. Erenas MM, Carrillo-Aguilera B, Cantrell K, et al. Real time monitoring of glucose in whole blood by smartphone. *Biosens Bioelectron* **2019**; 136: 47-52. <https://doi.org/10.1016/j.bios.2019.04.024>
19. Marinho OR, Lima MJA, Rocha FRP, Reis BF, Kamogawa MY. A greener, fast, and cost-effective smartphone-based digital image procedure for quantification of ethanol in distilled beverages. *Microchem J* **2019**; 147: 437-443. <https://doi.org/10.1016/j.microc.2019.03.054>
20. Salazar JH. Overview of Urea and Creatinine. *Lab Med* **2014**; 45: e19-e20. <https://doi.org/10.1309/LM920SBNZPJRGUT>
21. Kuswandi B, Mascini M. Enzyme Inhibition Based Biosensors for Environmental Monitoring. *Curr Enzym Inhib* **2005**; 1: 11-17.
22. Mao X, Du T, Meng L, acta TS-A chimica, 2015 undefined. Novel gold nanoparticle trimer reporter probe combined with dry-reagent cotton thread immunoassay device for rapid human ferritin test. Elsevier. <https://www.sciencedirect.com/science/article/pii/S0003267015008326>. Accessed May 30, 2019.
23. Wicaksono DH, Syazwani IN, Ratnarathorn N, et al. Cotton fiber-based assay with time-based microfluidic absorption sampling for point-of-care applications. *Bioanalysis* **2019**; 11: 855-873. <https://doi.org/10.4155/bio-2018-0190>
24. Cinti S, Cusenza R, Moscone D, Arduini F. Paper-based synthesis of Prussian Blue Nanoparticles for the development of whole blood glucose electrochemical biosensor. *Talanta* **2018**; 187: 59-64. <https://doi.org/10.1016/j.talanta.2018.05.015>
25. Chaudhari R, Joshi A, Srivastava R. pH and Urea Estimation in Urine Samples using Single Fluorophore and Ratiometric Fluorescent Biosensors. *Sci Rep* **2017**; 7: 5840. <https://doi.org/10.1038/s41598-017-06060-y>
26. Miller J, Miller J. *Statistics and Chemometrics for Analytical Chemistry*. 6th ed. Harlow: Pearson Education; **2010**.
27. Kellum JA. Determinants of blood pH in health and disease. *Crit Care* **2000**; 4: 6-14. <https://doi.org/10.1186/cc644>
28. Hosten AO. BUN and Creatinine. Butterworths; 1990. <http://www.ncbi.nlm.nih.gov/pubmed/21250147>. Accessed June 2, 2019.
29. Soni A, Surana RK, Jha SK. Smartphone based optical biosensor for the detection of urea in saliva. *Sensors Actuators B Chem* **2018**; 269: 346-353. <https://doi.org/10.1016/j.snb.2018.04.108>
30. Mahdiasanti IW, Sabarudin A, Sulistyarti H. Simultaneous determination of bun-creatinine as kidney function biomarkers in blood using a microfluidic paper-based analytical devices. *IOP Conf Ser Mater Sci Eng* **2019**; 546: 032019. <https://doi.org/10.1088/1757-899X/546/3/032019>